Philosophical Magazine
Publication details, including instructions for authors and subscription information:
http://www.tandfonline.com/loi/tphm20

Linking high- and low-temperature plasticity in bulk metallic glasses II: use of a log-normal barrier energy distribution and a mean-field description of high-temperature plasticity

P.M. Derlet[a] & R. Maaß[b]
[a] Condensed Matter Theory Group, Paul Scherrer Institut, CH-5232, Villigen PSI, Switzerland.
[b] Institute for Materials Physics, University of Göttingen, Friedrich-Hund-Platz 1, D-37077, Göttingen, Germany.
Published online: 10 Jul 2014.

To cite this article: P.M. Derlet & R. Maaß (2014): Linking high- and low-temperature plasticity in bulk metallic glasses II: use of a log-normal barrier energy distribution and a mean-field description of high-temperature plasticity, Philosophical Magazine, DOI: 10.1080/14786435.2014.932461

To link to this article: http://dx.doi.org/10.1080/14786435.2014.932461

Philosophical Magazine, 2014
http://dx.doi.org/10.1080/14786435.2014.932461

Taylor & Francis
Taylor & Francis Group

Linking high- and low-temperature plasticity in bulk metallic glasses II: use of a log-normal barrier energy distribution and a mean-field description of high-temperature plasticity

P.M. Derlet[a]* and R. Maaß[b]

[a]*Condensed Matter Theory Group, Paul Scherrer Institut, CH-5232 Villigen PSI, Switzerland;* [b]*Institute for Materials Physics, University of Göttingen, Friedrich-Hund-Platz 1, D-37077 Göttingen, Germany*

(*Received 13 November 2013; accepted 27 May 2014*)

A thermal activation model to describe the plasticity of bulk metallic glasses (Derlet and Maaß, Phil. Mag. 93 (2013) p.4232) which uses a distribution of barrier energies and some aspects of under-cooled liquid physics is developed further. In particular, a log-normal distribution is now employed to describe the statistics of barrier energies. A high-temperature mean-field description of homogeneous macroplasticity is then developed and is shown to be similar to a thermal activation picture employing a single characteristic activation energy and activation volume. In making this comparison, the activation volume is interpreted as being proportional to the average mean-square-value of the plastic shear strain magnitude within the material. Also, the kinetic fragility at the glass transition temperature is shown to represent the effective number of irreversible structural transformations available at that temperature.

Keywords: bulk metallic glasses; plastic deformation; theory

1. Introduction

The deformation properties of bulk metallic glasses are characterized by two temperature regimes [1]. At high temperatures, close to the glass transition temperature, BMGs deform homogeneously with the strain rate properties being reasonably well understood by thermally activated plastic flow. At lower temperatures, plasticity becomes heterogeneous and highly localized to shear-bands, resulting in limited ductility in tension and a few percent plastic strain prior to failure for some BMGs in compression. In this regime of temperatures, both athermal [2] and thermal [3–5] theories of plasticity have been proposed. In the early work of Turnbull and Cohen [6–8] these different regimes emerged as a result of two competing processes, one diffusional and one stress induced. Later, Spaepen [3] attributed the homogeneous regime as resulting from a steady state of free volume creation and diffusional related free volume annihilation. Heterogeneous flow on the other hand was dominated by free volume creation since annihilation became diffusion limited at low temperatures. That two distinct temperature scales exist was also recognized by Argon [4], who from the perspective of thermal activation developed two microscopic theories where at

*Corresponding author. Email: peter.derlet@psi.ch

high temperature, plasticity was mediated by small atomic reconfigurations that resulted in a localized shear strain event, and at lower temperature, a less local structural excitation occurs that was akin to the nucleation of a dislocation loop. Such mechanisms could give insight into both the observed high temperature homogeneous and low-temperature heterogeneous plasticity.

Sometime after this, high strain rate atomistic simulation revealed the generality of such local structural excitations, where the transition from homogeneous to heterogeneous plasticity (as a function of decreasing temperature or increasing strain rate) emerged from the degree of correlation between such localized activity [9–14]. Due to their high strain rates and stresses, both dynamic and static atomistic simulations primarily probe the athermal region of plasticity. Out of the earliest of this work by Falk and Langer [9] arose the concept of the Shear Transformation Zone (STZ) which was assumed to exist in regions of the material not so well relaxed – the so-called liquid like regions [12,15–17]. The corresponding structural transformations were assumed to be activated *athermally* once a critical stress had been reached. Such ideas developed into what is now called the effective temperature theories in which the quenched disorder well below the glass transition temperature is characterized by an effective temperature that describes the structural fluctuations within the material. See for example [2]. This approach has been quite successful in developing a quantitative understanding of experimental low-temperature deformation data.

It was recognized by Bouchbinder, Langer and Falk [18] that if one were to assume a thermal activation picture within the STZ framework [19,20], the density of such local structural excitations would have to be "improbably" large if the corresponding activation energies are in the realistic range of hundreds of kilojoule per mole (or electron volts per excitation). In going to an athermal picture, this difficulty was avoided and indeed STZs could now occur at quite dilute densities [18], a picture that is compatible with the distinct liquid like regions assumed to exist within the glass.

Understanding the nature of such STZs, or more generally localized structural excitations, has also been influenced by the physics of the under-cooled liquid regime, in which two distinct relaxation time-scales are evidenced: that of the slow α-relaxation and the fast β-relaxation processes first introduced by Goldstein [21] who considered the underlying potential energy landscape (PEL) of the under-cooled liquid. At temperatures near the glass transition and below, the α-relaxation processes rapidly increase their time-scale with the traditional viewpoint being that they freeze out of the structural dynamics in the amorphous solid regime [22]. Despite such an assumed freezing, the terminology of α- and β-relaxation has also been applied to the amorphous solid regime where the microscopic β processes mediate escape from the mega-basins of the elastic energy landscape of the α processes [23,24].

Following Goldstein, Stillinger's study of the under-cooled liquid PEL introduced the concept of the inherent structure (the meta-stable configurations associated with the minima of the potential energy) whose number depended exponentially on system size [25,26]. Historically, such a picture played a fundamental role in understanding the properties of the under-cooled liquid regime and its approach to glassiness [27,28]. More recently, Stillinger's work has been extended to the counting of higher order saddle-points, demonstrating that the available number of structural transformations will also scale exponentially with respect to volume [29,30]. This latter aspect was, in fact, also assumed in the early thermodynamic theories of Adam and Gibbs [31] and Kirkpatrick et al. [32] – see also the review article by Heuer [33].

The present work develops further the ideas of Refs. [34–36], which use the rational that an exponential number of available structural transformations supports the notion that thermal activation drives plasticity at temperatures at and also well below the glass transition temperature. Indeed, in these works, a thermal activation picture was developed in which the characteristic plastic rate with respect to an internal heterogeneous volume scale was determined from a distribution of α-relaxation barriers, whose number scales exponentially with the size of the heterogeneous volume and whose statistics is described by a distribution with extensive first and second cumulants. By doing this, the average time scale associated with plasticity at a particular temperature becomes intimately connected to the α-relaxation potential energy landscape which is thermally accessible at that temperature. Put in other words, the freezing out of α-relaxation processes is only complete at temperatures far below that of the glass transition temperature, and until this extreme regime is reached thermal activation remains the underlying phenomenon controlling macroscopic plasticity – a viewpoint that has been established experimentally for a variety of deformation geometries [1] including most recently that of shear band nucleation, propagation and arrest [37–39].

The present paper extends on the work done in Ref. [36] (which will be referred to as paper I) by (1) using a log-normal distribution to describe the statistics of the α-relaxation barrier energy landscape and (2) developing a mean-field description of thermally activated plasticity for the high temperature/low strain rate regime of homogeneous deformation. Section 2 gives a brief overview of the work done in paper I, Sections 3 and 4 develops the theory for the positive-valued log-normal distribution of barrier energies, Section 5 develops a mean-field description of plasticity suitable for the high-temperature homogeneous regime of deformation and Section 6 summarizes the theory, and discusses its assumptions and relationship to existing theories. Section 7 applies the theory to known experimental data for the well-studied BMG Vitreloy-1. In the discussion and conclusion, Section 8, two results are empahsized: (1) when comparing with the usual Arrhenius description of high-temperature homogeneous plasticity, the corresponding activation volume parameter is found to be equivalent to the variance of the internal slipped volume distribution, and (2) the fragility of the material is a measure of the number of structural transformations available at the glass transition temperature.

2. Brief summary of paper I

Paper I, Ref. [36], considered a characteristic time scale of irreversible structural transformation activity, $\tau_{\rm p}$, whose inverse is seen as a plastic transition rate below the glass transition temperature. Studying the resulting temperature and stress dependence of $\left[\tau_{\rm p}\right]^{-1}$ gave insight into the transition from elasticity to microplasticity. To determine $\left[\tau_{\rm p}\right]^{-1}$ it was recognized that, at a large enough length scale, BMGs are considered structurally homogeneous indicating that a sufficient amount of self-averaging occurs with respect to a shorter heterogeneous length scale. Thus, two length-scales naturally emerge which are realized through the homogeneous representative volume element (RVE) and the smaller heterogeneous volume elements. See Figure 1.

The plastic rate for an RVE is written as a sum of the N' heterogeneous volume plastic rates, $\left[\tau_{{\rm p},n}\right]^{-1}(T)$, within the RVE:

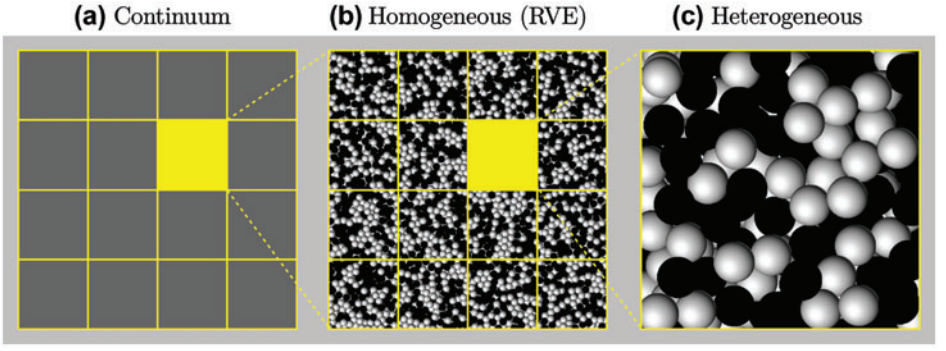

Figure 1. (colour online) Schematic of the assumed structural length scales of a bulk metallic glass where at a sufficiently large length scale of volume partitioning the material may be considered homogeneous, (a). Each such volume partition, referred to as the homogeneous representative volume element (RVE) with volume $V_{\rm RVE}$, will have the same rate of plastic activity, $\left[\tau_{\rm RVE,p}\right]^{-1}$. Each RVE may be further partitioned into N' heterogeneous volumes (of volume V_0), (b), where the nth heterogeneous volume element will have a particular rate of plastic activity, $\left[\tau_{{\rm p},n}\right]^{-1}$, (c).

$$\left[\tau_{\rm RVE,p}\right]^{-1}(T) = \sum_{n=1}^{N'} \left[\tau_{{\rm p},n}\right]^{-1}(T). \tag{1}$$

Equation (1) assumes that the heterogeneous volumes are statistically independent from each other. The right-hand side of the above equation may be rewritten as $N' \times \left[\tau_{\rm p}\right]^{-1}(T)$, where

$$\left[\tau_{\rm p}\right]^{-1}(T) = \frac{1}{N'} \sum_{n=1}^{N'} \left[\tau_{{\rm p},n}\right]^{-1}(T). \tag{2}$$

If $V_{\rm RVE} = N'V_0$, where $V_{\rm RVE}$ and V_0 are the respective characteristic RVE and heterogeneous volumes, then N' (and therefore $V_{\rm RVE}$) should be large enough such that $\left[\tau_{\rm RVE,p}\right]^{-1}(T)$ varies little from one RVE to another or, equivalently, Equation (2) should be a well-converged average.

Under the assumption of thermally activated plasticity, the plastic rate of the nth heterogeneous volume is written as a linear sum of the available thermally activated structural transformations:

$$\left[\tau_{\rm p,n}\right]^{-1}(T) = \sum_{i=1}^{M} \left[\tau_{{\rm p}0,ni}\right]^{-1}(T) \exp\left(-\frac{E_{{\rm p}0,ni}}{k_{\rm B}T}\right). \tag{3}$$

Here, $\left[\tau_{{\rm p}0,ni}\right]^{-1}(T)$ and $E_{{\rm p}0,ni}$ are the attempt rate and barrier energy for the ith irreversible structural transformation within the nth heterogeneous volume element, and M is the characteristic number of structural transitions within a heterogeneous volume element.

Equation (2) then can be rewritten as

$$\left[\tau_{\rm p}\right]^{-1}(T) = M \left\langle \left[\tau_{\rm p0}\right]^{-1}(T) \exp\left(-\frac{E_{\rm p0}}{k_{\rm B}T}\right) \right\rangle_{\left[\tau_{\rm p0}\right]^{-1}, E_{\rm p0}} \tag{4}$$

in which the average is now performed with respect to $\left[\tau_{\rm p0}\right]^{-1}(T)$ and $E_{\rm p0}$.

In terms of the underlying PEL, the simple (first order) expression of Equation (3) is only valid for thermally activated processes that do not multiply recross their energy barrier. This naturally leads to a coarse graining of the PEL, in which the barriers and (now diffusive) prefactors entering into Equation (3) underlie the collective microscopic activity that results in a lasting escape from a characteristic energy valley. By analogy to the under-cooled liquid PEL framework [23,33] where two distinct time scales occur – the "slow" α-relaxation and "fast" microscopic β-relaxation modes – the self-averaging of Equation (4) reduces (see paper I and Section 6 of the current work) to

$$\left[\tau_{\mathrm{p}}\right]^{-1} = \left[\tau_{\mathrm{p00}}\right]^{-1} \exp\left(-\frac{E_{\mathrm{p00}}}{k_{\mathrm{B}}T}\right) \times M\left\langle \exp\left(-\frac{E}{k_{\mathrm{B}}T}\right)\right\rangle. \tag{5}$$

Equation (5) consists of a diffusive attempt rate with a simple Arrhenius temperature dependence, representing the mediating β mode relaxation dynamics multiplied by a thermal factor whose temperature dependence will be derived from the statistical properties of the α-relaxation mode coarse grained PEL [35]. Its derivation assumes a statistical independence of the heterogeneous volumes and that there exists no statistically significant correlation between $\left[\tau_{\mathrm{p0},ni}\right]^{-1}(T)$ and $E_{\mathrm{p0},ni}$.

In paper I, the number of structural transformations available to each heterogeneous volume was assumed to scale exponentially with the number of atoms within V_0, giving $M = \exp(\alpha)$ where $\alpha = \overline{\alpha}N$ and N is the characteristic number of atoms within a heterogeneous volume. For a discussion on the meaning of $\overline{\alpha}$ see Ref. [36]. The right most average in Equation (5) is then evaluated via a distribution of barrier energies defined by an extensive first and second cumulant, and written as

$$M\left\langle \exp\left(-\frac{E}{k_{\mathrm{B}}T}\right)\right\rangle = \exp\left[-\frac{E(T) - TS(T)}{k_{\mathrm{B}}T}\right] = \exp\left[-\frac{F(T)}{k_{\mathrm{B}}T}\right]. \tag{6}$$

Here, $E(T)$ is interpreted as the temperature dependent internal barrier energy and $S(T)$ as the temperature dependent barrier entropy. Within this context, $F(T)$ is referred to as the free barrier energy. All of these quantities are extensive and $\exp(S(T)/k_{\mathrm{b}})$ gives the apparent number of structural transformations available at temperature T.

The separation of the free barrier energy into distinct internal barrier energy and barrier entropy contributions is not arbitrary, and arises due the left-hand side of Equation (6) having the mathematical structure of a partition function. Indeed by exploiting the mathematical apparatus of equilibrium statistical mechanics, Section 4 will develop the analytical expressions for both quantities (assuming a log-normal distribution of barrier energies) in which the barrier entropy represents the number of accessible structural transformations and the internal barrier energy represents the average (or apparent) barrier energy – both of which now are functions of temperature. In paper I, a Gaussian distribution was used giving closed form expressions for both $E(T)$ and $S(T)$. An important property of the above is that for a large enough N there exists a sharp crossover in behaviour where for, $F(T) > 0$, Equation (6) is negligible and for, $F(T) < 0$, it is exponentially large. Thus T_{c}, where $F(T_{\mathrm{c}}) = 0$, defines a critical temperature at which the plastic transition rate rapidly rises.

By assuming the application of a pure shear stress broadens the distribution via a quadratic increase in the variance (with respect to stress), all mentioned quantities, including T_{c}, gain a shear stress dependence. Via the assumption that at zero applied shear stress T_{c} corresponds approximately to the glass transition temperature, the stress dependence of T_{c} rises rapidly from zero at T_{g} as the temperature is lowered. At a temperature of approximately

0.8–$0.9T_g$, this temperature dependence weakens to an approximately linear behaviour upon further reduction in temperature. Interpreting $T_c(\sigma_c) = T_{\text{Deformation}}$ (where $T_{\text{Deformation}}$ is the temperature at which the deformation experiment is performed) as being the stress at which plasticity begins, an analytical form of yield stress vs. temperature that is valid in both the low- and high-temperature regimes could be developed, and could be fitted well to the available experimental data (see Figure 8 of [36]) of Lu et al. [40] and that shown in Johnson and Samwer [5]. Whilst a successful fit to low-temperature yield data is not new, the work of paper I has the virtue that the yield stress rapidly decreases as the temperature approaches T_g due to a change in barrier energy statistics rather than a change in mechanism.

3. The log-normal barrier energy distribution

In paper I, a normal distribution of barrier energies was considered and also a modified version such that the distribution would limit to zero at zero barrier energy. The present work will consider a log-normal distribution of barrier energies. This distribution has the desirable features of being a positive-valued distribution with independent first and second cumulants (average and variance) – a requirement of the current model. The log-normal distribution is given as

$$P(E) = \frac{1}{\sqrt{2\pi}E\sigma} \exp\left[-\frac{(\log E - \mu)^2}{2\sigma^2}\right] \tag{7}$$

where the first moment, $E^{(1)}$, is

$$E^{(1)} = \exp\left[\mu + \frac{1}{2}\sigma^2\right] \tag{8}$$

and the second moment, $E^{(2)}$, is defined via

$$\sigma^2 = \log\left[1 + \frac{E^{(2)} - \left(E^{(1)}\right)^2}{\left(E^{(1)}\right)^2}\right]. \tag{9}$$

In terms of $E^{(1)}$ and $E^{(2)}$, the distribution can be written as

$$P(E) = \frac{1}{\sqrt{2\pi}E\sqrt{2\log a}} \exp\left[-\frac{\log^2\left[\frac{Ea}{E^{(1)}}\right]}{4\log a}\right] \tag{10}$$

with

$$a = \frac{\sqrt{E^{(2)}}}{E^{(1)}}. \tag{11}$$

In paper I, it was argued that the barrier energy distribution shall have extensive first and second cumulants, that is, the barrier energy mean E_0 and variance δE_0^2 will be linear functions of the number of atoms, N, within the heterogeneous volume element. As in paper I, an over-lined quantity will represent the corresponding intensive variable giving $E_0 = N\overline{E}_0$ and $\delta E_0^2 = N\delta\overline{E}_0^2$. Thus, the first and second moments of Equation (10) will be

$$E^{(1)} = E_0 = N\overline{E}_0 \tag{12}$$

$$E^{(2)} = E_0^2 + \delta E_0^2 = N^2\overline{E}_0^2\left(1 + \frac{1}{N}\left(\frac{\delta\overline{E}_0}{\overline{E}_0}\right)^2\right) \tag{13}$$

resulting in

$$a = \sqrt{1 + \left(\frac{\delta E_0}{E_0}\right)^2} = \sqrt{1 + \frac{1}{N}\left(\frac{\delta\overline{E}_0}{\overline{E}_0}\right)^2}. \tag{14}$$

The log-normal distribution in the form of Equation (10) will now be used to obtain the average plastic rate per heterogeneous volume (Section 4) and, through a mean-field description of the internal stress, the average plastic strain rate per heterogeneous volume (Section 5) which can be considered as the flow equation for the high-temperature homogeneous deformation regime. More generally, it will be shown that the same central results of paper I are also obtained using a log-normal distribution of barrier energies.

4. The plastic transition rate via an analogy to statistical mechanics

The central mathematical challenge is to evaluate the final factor of Equation (5):

$$M\left\langle \exp\left(-\frac{E}{k_B T}\right)\right\rangle, \tag{15}$$

or, with respect to the barrier energy distribution,

$$M\int_0^\infty dE\, P(E)\exp\left(-\frac{E}{k_B T}\right). \tag{16}$$

The integral in Equation (16) is the generating function of the distribution, and for the Gaussian distribution considered in paper I it has a simple closed-form representation. For the log-normal distribution, such a straight forward avenue of calculation appears not to be available, however, the analogy to statistical mechanics derived in paper I provides a procedure for the evaluation of Equation (16). Indeed, Equation (15) can be viewed as

$$M\left\langle \exp\left(-\frac{E}{k_B T}\right)\right\rangle = \left\langle \sum_{i=1}^{M} \exp\left(-\frac{E_i}{k_B T}\right)\right\rangle, \tag{17}$$

where $\langle\cdots\rangle$ is an average over heterogeneous volumes. The right-hand side term has the structure of an environmentally averaged partition function allowing the mathematical problem to exploit the full apparatus of equilibrium statistical mechanics. To obtain a closed form expression of such a partition function, the microcanonical approach of Derrida [41] can be used to construct the corresponding free (barrier) energy. This procedure is now applied when the barrier energy distribution is taken as a log-normal distribution.

The average number of barrier energies between E and $E + dE$, $\langle\Omega(E)\rangle$, is given by

$$\langle\Omega(E)\rangle = M(E)dE = MP(E)dE, \tag{18}$$

where dE must be small enough to ensure a well-defined barrier energy but also large enough so that $\langle\Omega(E)\rangle$ is a smooth function of E (see Ref. [41] for a related discussion). For

a sufficiently large heterogeneous volume, fluctuations in Equation (18) become small and $\langle\Omega(E)\rangle$ becomes a statistically meaningful quantity, allowing for a corresponding barrier entropy to be defined via $S(E) = k_{\mathrm{B}} \log\langle\Omega(E)\rangle$. Doing this for the log-normal distribution, Equation (10), results in the barrier entropy:

$$S(E) = k_{\mathrm{B}} \left(\alpha - \frac{\log^2 \left[\frac{Ea}{E_0} \right]}{4 \log a} + \log \left[\frac{1}{\sqrt{2 \log a}} \right] + \log \left[\frac{dE}{\sqrt{2\pi}\, E} \right] \right). \tag{19}$$

To obtain the internal barrier energy and entropy as functions of temperature, an analogy to the thermodynamic definition,

$$\frac{dS(E)}{dE} = \frac{1}{T}, \tag{20}$$

is applied to Equation (19), giving

$$\log \left[\frac{E(T)a}{E_0} \right] = -2 \log a \left(1 + \frac{E(T)}{k_{\mathrm{B}} T} \right). \tag{21}$$

A solution to the above with respect to $E(T)$ is obtained via the Lambert W-function giving

$$E(T) = k_{\mathrm{B}} T \frac{1}{2 \log a} W \left[\frac{E_0}{k_{\mathrm{B}} T} \frac{2 \log a}{a^3} \right]. \tag{22}$$

Equation (22) gives the internal barrier energy as a function of temperature and its substitution into Equation (19) gives the barrier entropy as a function of temperature:

$$S(T) = k_{\mathrm{B}} \left(\alpha - \frac{1}{2} \left(\log \left[2\sqrt{a} \log a \right] + 3 \log \left[\frac{E(T)}{E_0} \right] + \frac{1}{2 \log a} \log \left[\frac{E(T)}{E_0} \right]^2 \right) \right). \tag{23}$$

In the above, the term containing dE in Equation (19) has been taken as $\log[dE/(\sqrt{2\pi}E)] = \log[\langle E\rangle/E] + \log[dE/(\sqrt{2\pi}\langle E\rangle)] \sim \log[\langle E\rangle/(\sqrt{2\pi}E)]$. This approximation will be discussed in the proceeding paragraphs.

Equations (22) and (23) give the free barrier entropy, $F(T) = E(T) - TS(T)$, and therefore the final form of Equation (17) as

$$M \left\langle \exp\left(-\frac{E}{k_{\mathrm{B}} T} \right) \right\rangle = \exp \left[-\frac{F(T)}{k_{\mathrm{B}} T} \right]. \tag{24}$$

Substitution of this back into Equation (5) gives

$$\left[\tau_{\mathrm{p}}\right]^{-1} = \left[\tau_{\mathrm{p00}}\right]^{-1} \exp\left(\frac{S(T)}{k_{\mathrm{B}}} \right) \exp\left(-\frac{E_{\mathrm{p00}} + E(T)}{k_{\mathrm{B}} T} \right) \tag{25}$$

where $E_{\mathrm{p00}} + E(T)$ can be viewed as the apparent barrier energy and the exponential involving $S(T)$ as the number of thermally accessible structural transformations available to the heterogeneous volume. Using Equations (12)–(14), the $N \to \infty$ limit of $F(T)$, gives

$$\lim_{N\to\infty} \frac{F(T)}{N} = k_{\mathrm{B}} T \left(\frac{E_0^2}{\delta \overline{E}_0^2} \frac{1}{2} \left(\log \left[\frac{k_{\mathrm{B}} T \overline{E}_0}{\delta \overline{E}_0^2} W \left[\frac{\delta \overline{E}_0^2}{k_{\mathrm{B}} T \overline{E}_0} \right] \right]^2 + 2W \left[\frac{\delta \overline{E}_0^2}{k_{\mathrm{B}} T \overline{E}_0} \right] \right) - \overline{\alpha} \right) \tag{26}$$

demonstrating that for large enough heterogeneous volumes the free barrier energy is an extensive quantity as is the case of the a Gaussian distribution. Indeed by expanding those terms involving the Lambert W-function as a Taylor series to second order in $\delta\overline{E}_0^2/(k_{\mathrm{B}}T\overline{E}_0)$ recovers a central result of paper I:

$$\lim_{N\to\infty}\frac{F(T)}{N}\simeq k_{\mathrm{B}}T\left(\frac{\overline{E}_0}{k_{\mathrm{B}}T}-\left(\frac{\delta\overline{E}_0}{k_{\mathrm{B}}T}\right)^2\right)-k_{\mathrm{B}}T\overline{\alpha}. \tag{27}$$

That is, for a narrow enough distribution (set by $\delta\overline{E}_0$), the free barrier energy limits to that obtained for a Gaussian distribution of barrier energies as derived in Paper I. This is compatible with the fact that for a small enough $\delta\overline{E}_0$, the log normal distribution limits to a Gaussian distribution. Equation (27) has the virtue that it leads to a simple analytic solution to $F(T_{\mathrm{c}})=0$ for the critical temperature at which significant plastic activity can be expected (see Equation (11) of Ref. [36]).

Equation (26) will be used for further development since it is only at this limit that the right most term in Equation (19) becomes negligible and can be ignored. Indeed Derrida [41] has argued that $dE\sim N^{\zeta}$ where $\zeta<1$. Moreover Equation (26) affords a simpler mathematical formalism which is more easily comparable to the normal distribution used in paper I. Reabsorbing the factor N into the free barrier energy gives $F(T)=E(T)-TS(T)$ as

$$F(T)=k_{\mathrm{B}}T\left(\frac{E_0^2}{\delta E_0^2}\frac{1}{2}\left(\log\left[\frac{k_{\mathrm{B}}TE_0}{\delta E_0^2}W\left[\frac{\delta E_0^2}{k_{\mathrm{B}}TE_0}\right]\right]^2+2W\left[\frac{\delta E_0^2}{k_{\mathrm{B}}TE_0}\right]\right)-\alpha\right) \tag{28}$$

with

$$E(T)=\frac{k_{\mathrm{B}}TE_0^2}{\delta E_0^2}W\left[\frac{\delta E_0^2}{k_{\mathrm{B}}TE_0}\right] \tag{29}$$

and

$$S(T)=k_{\mathrm{B}}\left(\alpha-\frac{E_0^2}{\delta E_0^2}\frac{1}{2}\log\left[\frac{k_{\mathrm{B}}TE_0}{\delta E_0^2}W\left[\frac{\delta E_0^2}{k_{\mathrm{B}}TE_0}\right]\right]^2\right). \tag{30}$$

Thus, the plastic strain rate (Equation (5)) becomes

$$\left[\tau_{\mathrm{p}}\right]^{-1}=\left[\tau_{\mathrm{p00}}\right]^{-1}\exp\left(-\frac{E_{\mathrm{p00}}+F(T)}{k_{\mathrm{B}}T}\right) \tag{31}$$

with $F(T)$ being given by Equation (28). Once again, it is emphasized that the separation of Equation (28) into Equations (29) and (30) into, respectively, an internal barrier energy and barrier entropy is not arbitrary, and follows from the structure of Equation (15) being similar to that of the partition function of equilibrium statistical mechanics.

5. Macroscopic plasticity – a mean-field approach

Paper I considered only the characteristic escape rate from a mega-basin and could only describe the onset of the transition away from elasticity. For subsequent plastic strain evolution, the new mega-basin into which the material enters is of importance giving the final irreversible structural transformation associated with the escape. Under zero load conditions,

the material traverses (at a long enough time-scale and high enough temperature) a series of mega-basins and the internal plastic strain fluctuates accordingly. Due to elastic interaction, these local plastic strain fluctuations correspond to internal stress fluctuations and therefore an elastic potential energy landscape. In the regime of an amorphous solid, it is such a coarse grained elastic potential energy landscape which underlies the alpha energy landscape and therefore the heterogeneity of the material. Due to thermal fluctuations, upon exiting one mega-basin the material will be stochastically biased towards choosing a new mega-basin which minimizes the total elastic energy. This situation does not change upon application of a load, however those structural transformations that can reduce the elastic energy of a particular deformation geometry will become more likely. Thus, plastic deformation will evolve the internal stress state of the material and thus its alpha energy landscape.

In terms of heterogeneous volume partitioning, the above picture indicates the primary interaction between heterogeneous volumes will be of elastic origin. The inclusion of such interactions may be done via the Eshelby construction. Here, the goal is to calculate the change in total elastic energy arising from a local plastic strain increment within a particular heterogeneous volume (the nth) of volume V_0. In the Eshelby construction [42], this is done by removing from the amorphous matrix the heterogeneous volume in which the plastic event has occurred, and allowing it to relax to a stress free state given by $\varepsilon_{\mathrm{T}}^{\mu\nu}$. The heterogeneous volume is then deformed elastically to return it to its original shape via the corresponding elastic strain $-\varepsilon_{\mathrm{T}}^{\mu\nu}$ and re-inserted into the matrix. At this point, the particular heterogeneous volume (the inclusion) has an inclusion stress derived from Hooke's law equal to $\sigma_{\mathrm{T}}^{\mu\nu}$ whilst the surrounding matrix is stress free. The combined system is then allowed to relax to an equilibrium internal stress configuration reducing the inclusion stress by $\sigma_{\mathrm{C}}^{\mu\nu}$. Eshelby has then shown that the total change in elastic energy is given by $V_0/2\varepsilon_{\mathrm{T}}^{\mu\nu}(\sigma_{\mathrm{T}}^{\mu\nu} - \sigma_{\mathrm{C}}^{\mu\nu} - \sigma_{\mathrm{E},n}^{\mu\nu})$ where $\sigma_{\mathrm{E},n}^{\mu\nu}$ is an additional external stress (to the nth heterogeneous volume). Here, and throughout the text, repeated indices are summed.

How does the above discussion affect the distribution of energy barriers? In paper I, upon application of a *pure* shear stress, the barrier energy distribution was assumed to broaden since any local structural transformation (identified at zero load) would have equal chance of doing work for or against the applied load. The above Eshelby construction now allows this approach to be placed in a more quantitative framework. A particular energy barrier may be expressed as the sum of a core contribution not describable via elasticity, E_{ni}^{core}, and an Eshelby term evaluated at the transitory plastic strain,[1] $\varepsilon_{*\mathrm{T},ni}^{\mu\nu}$, associated with the saddle-point of the coarse grained α landscape:

$$E_{ni} = E_{ni}^{\mathrm{core}} + \frac{1}{2} V_0 \varepsilon_{*\mathrm{T},ni}^{\mu\nu} \left(\sigma_{\mathrm{T}}^{\mu\nu} - \sigma_{\mathrm{C}}^{\mu\nu} - \sigma_{\mathrm{E},n}^{\mu\nu} \right). \tag{32}$$

When considering E_{ni}^{core} and $\varepsilon_{*\mathrm{T},ni}^{\mu\nu}$ as random variables the above equation can just as well be written as

$$E_{ni} = E_{ni}^{0} - \frac{1}{2} V_0 \varepsilon_{*\mathrm{T},ni}^{\mu\nu} \sigma_{\mathrm{E},n}^{\mu\nu} \tag{33}$$

where now the random variables are the (zero external load) barrier energy, $E_{ni}^{0} = E_{ni}^{\mathrm{core}} + 1/2 V_0 \varepsilon_{*\mathrm{T},ni}^{\mu\nu} \left(\sigma_{\mathrm{T}}^{\mu\nu} - \sigma_{\mathrm{C}}^{\mu\nu} \right)$ and $\varepsilon_{*\mathrm{T},ni}^{\mu\nu}$. For each structural transformation, the core term is expected to have some stress dependence which is much weaker than that of the elastic energy term. For a pure external shear stress, the elastic energy term is equally likely to be either positive or negative (see Equation (47) which is the restricted case of plane strain)

– a result that gives rational to the assumption of a broadening barrier distribution upon application of a pure shear stress.

The transition rate associated with exiting the current mega-basin via the nith structural transformation at an external stress, $\sigma^{\mu\nu}_{\mathrm{E},n}$, is therefore given by a generalization to the summand of Equation (3):

$$\left[\tau_{\mathrm{p0},ni}\right]^{-1}(T)\exp\left(-\frac{E_{\mathrm{p0},ni}-\frac{1}{2}V_0\varepsilon^{\mu\nu}_{*\mathrm{T},ni}\sigma^{\mu\nu}_{\mathrm{E},n}}{k_{\mathrm{B}}T}\right)=\left[\tau_{\mathrm{p0},ni}\right]^{-1}(T)\exp\left(-\frac{E_{\mathrm{p0},ni}(\sigma^{\mu\nu}_{\mathrm{E},n})}{k_{\mathrm{B}}T}\right). \tag{34}$$

This equation however does not give the transition rate to the final mega-basin, since the transitory plastic strain $\varepsilon^{\mu\nu}_{*\mathrm{T},ni}$ associated with the saddle-point should not at all be related to the final plastic strain state associated with this final mega-basin, $\varepsilon^{\mu\nu}_{\mathrm{T}}$.

To include this latter aspect, it is recognized that upon exiting its current mega-basin the system is in an excited state which rapidly relaxes to achieve a *local* thermal equilibrium that selects a new mega-basin according to Boltzmann statistics. Assuming that the only change in energy in going from one mega-basin to another is the change in elastic energy, the associated transition rate becomes

$$\left[\tau_{\mathrm{p0},ni}\right]^{-1}(T)\exp\left(-\frac{E_{\mathrm{p0},ni}(\sigma^{\mu\nu}_{\mathrm{E},n})+\frac{1}{2}V_0\varepsilon^{\mu\nu}_{\mathrm{T}}\left(\sigma^{\mu\nu}_{\mathrm{T}}-\sigma^{\mu\nu}_{\mathrm{C}}-\sigma^{\mu\nu}_{\mathrm{E},n}\right)}{k_{\mathrm{B}}T}\right). \tag{35}$$

Summing over all such irreversible structural transformations within the nth heterogeneous volume, the strain rate for nth heterogeneous volume can be written as

$$\dot{\varepsilon}^{\mu\nu}_{n}(T)=\sum_{i=1}^{M}\varepsilon^{\mu\nu}_{\mathrm{T},ni}\left[\tau_{\mathrm{p0},ni}\right]^{-1}\exp\left[-\frac{E_{\mathrm{p0},ni}(\sigma^{\mu\nu}_{\mathrm{E},n})+\frac{1}{2}V_0\varepsilon^{\mu\nu}_{\mathrm{T},ni}\left(\sigma^{\mu\nu}_{\mathrm{T},ni}-\sigma^{\mu\nu}_{\mathrm{C},ni}-\sigma^{\mu\nu}_{\mathrm{E},n}\right)}{k_{\mathrm{B}}T}\right]. \tag{36}$$

The above equation employs the usual thermal activation framework in which the strain rate is the product of the rate of occurrence of a plastic event and the associated plastic strain increment. The strain rate for the RVE is therefore

$$\dot{\varepsilon}^{\mu\nu}_{\mathrm{RVE}}(T)=\frac{V_0}{V_{\mathrm{RVE}}}\sum_{n=1}^{N'}\dot{\varepsilon}^{\mu\nu}_{n}(T). \tag{37}$$

Since $V_0/V_{\mathrm{RVE}}=1/N'$, the above equation becomes

$$\dot{\varepsilon}^{\mu\nu}_{\mathrm{RVE}}(T)=\frac{1}{N'}\sum_{n=1}^{N'}\sum_{i=1}^{M}\varepsilon^{\mu\nu}_{\mathrm{T},ni}\left[\tau_{\mathrm{p0},ni}\right]^{-1}\times\exp\left[-\frac{E_{\mathrm{p0},ni}(\sigma^{\mu\nu}_{\mathrm{E},n})+\frac{1}{2}V_0\varepsilon^{\mu\nu}_{\mathrm{T},ni}\left(\sigma^{\mu\nu}_{\mathrm{T},ni}-\sigma^{\mu\nu}_{\mathrm{C},ni}-\sigma^{\mu\nu}_{\mathrm{E},n}\right)}{k_{\mathrm{B}}T}\right]. \tag{38}$$

The elastic relaxation associated with the ith plastic event, within and surrounding the nth heterogeneous volume, results in $\sigma^{\mu\nu}_{\mathrm{C},ni}$ and an extended stress field felt by other nearby and distant heterogeneous volumes (through their own $\sigma^{\mu\nu}_{\mathrm{E}}$). From this latter perspective $\sigma^{\mu\nu}_{\mathrm{C},ni}$ can be viewed as a self-stress contribution to the elastic energy of the plastic event.

The spatial dependence of these stress contributions depend in a non-trivial way on $\sigma_{\mathrm{T}}^{\mu\nu}$ and must be calculated numerically (see e.g. the book of Mura [43] and Refs. [42,44]). It is in this way, that elastic interactions between heterogeneous volumes may be naturally introduced. In addition, the $\sigma_{\mathrm{E},n}^{\mu\nu}$ may contain a global applied external stress component written as $\sigma^{\mu\nu}$ giving $\dot{\varepsilon}_{\mathrm{RVE}}^{\mu\nu}(T) = \dot{\varepsilon}_{\mathrm{RVE}}^{\mu\nu}(T, \sigma^{\mu\nu})$. It is noted that Equation (38) still embodies the assumption of the statistical independence of each heterogeneous volume, however now the statistics of each is biased by the local stress arising via elasticity from all other heterogeneous volumes.

Thus for each heterogeneous volume, $\sigma_{\mathrm{E},n}^{\mu\nu}$ arises from an external applied stress plus an internal stress arising from the elastic interaction between the plastic events from all other heterogeneous volumes. Such a formalism has been considered by Bulatov and Argon [44–46] in their development of a thermal activation model for the plasticity of glasses, and more recently using the finite-element method by Homer and Schuh [47–49]. In the present work, a mean-field approach will be taken which exploits the fact that the local contribution to $\sigma_{\mathrm{E},n}^{\mu\nu}$ arising from other heterogeneous volumes will on average equal zero, giving $\sigma_{\mathrm{E},n}^{\mu\nu} = \sigma^{\mu\nu}$. For an assumed isotropic elasticity, $\varepsilon_{\mathrm{T},ni}^{\mu\nu}(\sigma_{\mathrm{T},ni}^{\mu\nu} - \sigma_{\mathrm{C},ni}^{\mu\nu})$ will equal $4V_0(G - \delta G_{ni})\gamma_{\mathrm{T},ni}^2$ where $\gamma_{\mathrm{T},ni}$ will be the shear strain magnitude of the plastic event and G is the appropriate bulk isotropic shear modulus for the system. δG_{ni} embodies the elastic relaxation of the plastic strain event and will be different for each plastic event. Within the current mean-field approach this will be absorbed into G resulting in an effective bulk shear modulus of the system.

These approximations afford a simple average with respect to heterogeneous volumes resulting in Equation (38) becoming

$$\dot{\varepsilon}_{\mathrm{RVE}}^{\mu\nu}\left(T, \sigma^{\mu\nu}\right) = M\left\langle \varepsilon_{\mathrm{T}}^{\mu\nu}\left[\tau_{\mathrm{p0}}\right]^{-1} \exp\left[-\frac{E_{\mathrm{p0}} + 2V_0 G\gamma_{\mathrm{T}}^2 - \frac{1}{2}V_0\varepsilon_{\mathrm{T}}^{\mu\nu}\sigma^{\mu\nu}}{k_{\mathrm{B}}T}\right]\right\rangle, \tag{39}$$

in which the average is performed with respect to $\varepsilon_{\mathrm{T}}^{\mu\nu}$, τ_{p0} and E_{p0}. Since there should be no correlation between the strain increment $\varepsilon_{\mathrm{T}}^{\mu\nu}$ and the parameters τ_{p0} and E_{p0} associated with the escape of a particular mega-basin (since each strain state is always accessible), the above average with respect to $\varepsilon_{\mathrm{T}}^{\mu\nu}$ may be performed independently from τ_{p0} and E_{p0}, giving,

$$\begin{aligned}
&\dot{\varepsilon}_{\mathrm{RVE}}^{\mu\nu}\left(T, \sigma^{\mu\nu}\right) \\
&\quad = \left\langle \varepsilon_{\mathrm{T}}^{\mu\nu} \exp\left[\frac{-2V_0 G\gamma_{\mathrm{T}}^2 + \frac{1}{2}V_0\varepsilon_{\mathrm{T}}^{\mu\nu}\sigma^{\mu\nu}}{k_{\mathrm{B}}T}\right]\right\rangle_{\varepsilon_{\mathrm{T}}^{\mu\nu}} M\left\langle \left[\tau_{\mathrm{p0}}\right]^{-1} \exp\left[-\frac{E_{\mathrm{p0}}}{k_{\mathrm{B}}T}\right]\right\rangle_{\tau_{\mathrm{p0}}, E_{\mathrm{p0}}} \\
&\quad = \left\langle \varepsilon_{\mathrm{T}}^{\mu\nu} \exp\left[\frac{-2V_0 G\gamma_{\mathrm{T}}^2 + \frac{1}{2}V_0\varepsilon_{\mathrm{T}}^{\mu\nu}\sigma^{\mu\nu}}{k_{\mathrm{B}}T}\right]\right\rangle_{\varepsilon_{\mathrm{T}}^{\mu\nu}} \left[\tau_{\mathrm{p}}\right]^{-1}\left(T, \sigma^{\mu\nu}\right).
\end{aligned} \tag{40}$$

In the last equality, $\left[\tau_{\mathrm{p}}\right]^{-1}(T, \sigma^{\mu\nu})$ is given by Equation (5). Here, the stress dependence is gained via the assumed quadratic dependence on pure shear stress of the variance of the barrier energy distribution [36]:

$$\delta E_0(\sigma) = \delta E_0(\sigma = 0)\left(1 + \left(\frac{\sigma}{\sigma_0}\right)^2\right), \tag{41}$$

where σ_0 becomes a fitting parameter. Equation (33) and the associated text now give this assumption a theoretical basis. In what follows, this expression is re-written as

$$\delta E_0(\sigma) = \delta E_0(\sigma = 0) + \delta E_\sigma \left(\frac{\sigma}{G}\right)^2, \tag{42}$$

where the new fitting parameter is now δE_σ and G is an appropriate value for the bulk shear modulus.

Treating, $\varepsilon_{\mathrm{T}}^{\mu\nu}$, τ_{p0} and E_{p0} as independent stochastic variables has the consequence that the barrier energy is, on average, not correlated with the magnitude of the resulting plastic strain increment. This scenario, again, appeals to the notion of an exponentially large diversity of possible structural excitation. Moreover, numerical evidence in simple Lennard Jones structural glasses exists, demonstrating that the strain associated in traversing a nearby local PEL minima does not at all correlate with the height of the intermediate saddle-point (barrier) energy [50,51]. A similar recent study has also demonstrated a very weak dependence between prefactor (derived from harmonic transition state theory) and energy barrier [52].

The plastic strain average in Equation (40) may be written as

$$\begin{aligned}\left\langle \varepsilon_{\mathrm{T}}^{\mu\nu} \exp\left[\frac{-2V_0 G\gamma_{\mathrm{T}}^2 + \frac{1}{2}V_0 \varepsilon_{\mathrm{T}}^{\mu\nu}\sigma^{\mu\nu}}{k_{\mathrm{B}}T}\right]\right\rangle_{\varepsilon_{\mathrm{T}}^{\mu\nu}} \\ = \frac{\partial}{\partial\left[\frac{\frac{1}{2}V_0\sigma^{\mu\nu}}{k_{\mathrm{B}}T}\right]}\left\langle \exp\left[\frac{-2V_0 G\gamma_{\mathrm{T}}^2 + \frac{1}{2}V_0 \varepsilon_{\mathrm{T}}^{\mu\nu}\sigma^{\mu\nu}}{k_{\mathrm{B}}T}\right]\right\rangle_{\varepsilon_{\mathrm{T}}^{\mu\nu}}\end{aligned} \tag{43}$$

and therefore the goal is to calculate

$$\left\langle \exp\left[\frac{-2V_0 G\gamma_{\mathrm{T}}^2 + \frac{1}{2}V_0 \varepsilon_{\mathrm{T}}^{\mu\nu}\sigma^{\mu\nu}}{k_{\mathrm{B}}T}\right]\right\rangle_{\varepsilon_{\mathrm{T}}^{\mu\nu}}. \tag{44}$$

To evaluate this average further, the two-dimensional case of plane strain will be considered involving only an external pure shear stress component:

$$\sigma^{\mu\nu} = \begin{pmatrix} 0 & \sigma & 0 \\ \sigma & 0 & 0 \\ 0 & 0 & 0 \end{pmatrix}. \tag{45}$$

Under these constraints, the characteristic shear strain matrix takes the form

$$\gamma_{\mathrm{T}} \begin{pmatrix} 2\sin\theta_{\mathrm{T}}\cos\theta_{\mathrm{T}} & \cos 2\theta_{\mathrm{T}} & 0 \\ \cos 2\theta_{\mathrm{T}} & -2\sin\theta_{\mathrm{T}}\cos\theta_{\mathrm{T}} & 0 \\ 0 & 0 & 0 \end{pmatrix} \tag{46}$$

giving

$$\varepsilon_{\mathrm{T}}^{\mu\nu}\sigma^{\mu\nu} = 2\gamma_{\mathrm{T}}\sigma\cos 2\theta_{\mathrm{T}}. \tag{47}$$

Thus, all possible plastic strain increments are defined by an orientation angle θ_{T} and a plastic shear strain magnitude γ_{T}. Due to the exponentially large number of plastic strain increments available and the lack of a preferred direction, the random variable θ_{T} is assumed to be derived from a uniform distribution ranging from $\theta_{\mathrm{T}} = 0$ to $\theta_{\mathrm{T}} = \pi$. On the other

hand, for reasonable values of the shear strain magnitude, the distribution for γ_{T} is expected to be bounded. Presently (and for mathematical simplicity), the distribution is assumed to be a normal distribution centred on zero with standard deviation $\delta\gamma$. It is acknowledged that other distributions are also feasible. With these assumptions, Equation (44) becomes

$$\left\langle \exp\left[\frac{-2V_0G\gamma_{\mathrm{T}}^2+\frac{1}{2}V_0\varepsilon_{\mathrm{T}}^{\mu\nu}\sigma^{\mu\nu}}{k_{\mathrm{B}}T}\right]\right\rangle_{\theta_{\mathrm{T}},\gamma_{\mathrm{T}}} = \exp\left[\left(\frac{V_0\delta\gamma'\sigma}{2k_{\mathrm{B}}T}\right)^2\right]\mathrm{I}_0\left[\left(\frac{V_0\delta\gamma'\sigma}{2k_{\mathrm{B}}T}\right)^2\right]. \tag{48}$$

where $\mathrm{I}_n(x)$ is the modified Bessel function of order n and

$$\left(\delta\gamma'\right)^2 = \frac{\delta\gamma^2}{1+\frac{4V_0G\delta\gamma^2}{k_{\mathrm{B}}T}} \simeq \delta\gamma^2. \tag{49}$$

In Section 7, the latter approximation will be shown to be valid for temperatures close to the glass transition temperature.

Using Equation (43), this finally gives the strain rate per heterogeneous volume as

$$\begin{aligned}\dot{\gamma}_{\mathrm{RVE}}(T,\sigma) = 2\left(\frac{V_0\delta\gamma^2\sigma}{2k_{\mathrm{B}}T}\right)\exp\left[\left(\frac{V_0\delta\gamma\sigma}{2k_{\mathrm{B}}T}\right)^2\right] \\ \times\left(\mathrm{I}_0\left[\left(\frac{V_0\delta\gamma\sigma}{2k_{\mathrm{B}}T}\right)^2\right]+\mathrm{I}_1\left[\left(\frac{V_0\delta\gamma\sigma}{2k_{\mathrm{B}}T}\right)^2\right]\right) \\ \times\left[\tau_{\mathrm{p}}\right]^{-1}\left(T,\sigma^{\mu\nu}\right)\end{aligned} \tag{50}$$

Using Equation (31) and writing, $\delta\gamma = \delta\gamma_0/V_0$, this reduces to

$$\begin{aligned}\dot{\gamma}_{\mathrm{RVE}}(T,\sigma) = \delta\dot{\gamma}_0\left(\frac{\delta\Omega\sigma}{k_{\mathrm{B}}T}\right)\exp\left[\left(\frac{\delta\Omega\sigma}{2k_{\mathrm{B}}T}\right)^2\right]\left(\mathrm{I}_0\left[\left(\frac{\delta\Omega\sigma}{2k_{\mathrm{B}}T}\right)^2\right]+\mathrm{I}_1\left[\left(\frac{\delta\Omega\sigma}{2k_{\mathrm{B}}T}\right)^2\right]\right) \\ \times\exp\left[-\frac{E_{\mathrm{p00}}+F(T,\sigma)}{k_{\mathrm{B}}T}\right]\end{aligned} \tag{51}$$

where

$$\delta\Omega = \frac{\delta\gamma_0}{2} \tag{52}$$

and

$$\delta\dot{\gamma}_0 = \frac{2\delta\gamma_0}{V_0\tau_{\mathrm{p00}}}. \tag{53}$$

Equation (51), written explicitly in terms of the internal barrier energy and barrier entropy, becomes

$$\begin{aligned}\dot{\gamma}_{\mathrm{RVE}}(T,\sigma) = \delta\dot{\gamma}_0\exp\left(\frac{S(T,\sigma)}{k_{\mathrm{B}}T}\right) \\ \times\left(\frac{\delta\Omega\sigma}{k_{\mathrm{B}}T}\right)\exp\left[\left(\frac{\delta\Omega\sigma}{2k_{\mathrm{B}}T}\right)^2\right]\left(\mathrm{I}_0\left[\left(\frac{\delta\Omega\sigma}{2k_{\mathrm{B}}T}\right)^2\right]+\mathrm{I}_1\left[\left(\frac{\delta\Omega\sigma}{2k_{\mathrm{B}}T}\right)^2\right]\right) \\ \times\exp\left[-\frac{E_{\mathrm{p00}}+E(T,\sigma)}{k_{\mathrm{B}}T}\right].\end{aligned} \tag{54}$$

The above equation should be compared to the early thermal activation models grounded on the work of Spaepen [3] and Argon [4], which for homogeneous plastic deformation in the vicinity of the glass transition temperature is usually taken as [1,24]

$$\dot{\gamma} = \alpha_{\mathrm{ta}} \nu_{\mathrm{ta}} \gamma_{\mathrm{ta}} \exp\left[-\frac{Q_{\mathrm{ta}}}{k_{\mathrm{B}} T}\right] \sinh\left[\frac{V_{\mathrm{ta}} \sigma}{k_{\mathrm{B}} T}\right] \tag{55}$$

where α_{ta} contains various quantities including the fraction of volume available to deformation, ν_{ta} is the attempt frequency, γ_{ta} is the characteristic strain, Q_{ta} is the activation energy and V_{ta} is the activation volume. Comparison of Equations (54) and (55) suggest that $\delta\dot{\gamma}_0$ can be viewed as a characteristic strain rate ($=\nu_{\mathrm{ta}}\gamma_{\mathrm{ta}}$ of Equation (55)), $\exp\left[S(T,\sigma)/k_{\mathrm{B}}\right]$ as a temperature and stress dependent number of available structural transformations, $E_{\mathrm{p00}} + E(T,\sigma)$ as a temperature and stress dependent activation energy, and $\delta\Omega$ as an activation volume. This latter interpretation is motivated by the term $x\exp(x^2)(\mathrm{I}_0[x^2] + \mathrm{I}_1[x^2])$ being qualitatively similar to $\sinh(x)$, with both limiting to a linear function for small x.

The present theory relies on a number of simplifying assumptions which will be summarized and addressed in the following section. Whilst the model has a number of quite different physical assumptions when compared to earlier high-temperature thermal activation models, the mean-field prediction of the average strain rate as a function of temperature and stress in the high temperature/low strain rate regime does not operationally differ from these early models. This observation will be shown in more detail in the Section 7, when the model is fitted to actual experimental data.

6. Model summary and assumptions, and comparison to other work

The main aspects of the present model are now listed in point form:

(1) The central result of the present model is entailed by Equation (38). This equation gives the instantaneous plastic rate of the RVE as the sum of those plastic rates originating from each possible structural transformation in each heterogeneous volume. All heterogeneous volumes elastically interact with each other experiencing an external stress, $\sigma^{\mu\nu}_{\mathrm{E},n}$, which is the sum of an externally applied homogeneous stress and an internal stress originating from the other heterogeneous volumes. Equation (38) contains no averaging, and could form the basis of a numerical approach along the lines of Bulatov and Argon [44–46] or Homer and Schuh [47–49]. This latter aspect will be discussed in Section 8.

(2) The physical picture that Equation (38) embodies is that, upon exiting (via thermal activation) a mega-basin, the system rapidly reaches local thermal equilibrium and chooses a new mega-basin stochastically according to the Boltzmann statistics of the available elastic energy landscape. In going from one mega-basin to another, it is assumed that the change in energy of the system is due only to the change in elastic energy. Two quite separate dependencies on the external applied stress arise, that of the coarse grained energy barrier distribution and that associated with the selection of the new mega-basin.

(3) For the treatment of high temperature and/or low strain rate homogeneous plasticity, a mean-field picture is developed. Under this assumption, the heterogeneous volumes no longer interact, allowing for a simple averaging over the heterogeneous volumes contained within the RVE (as done in paper I). The averaging is done

by assuming the statistical independence of the three parameters defining each irreversible structural transformation: $\varepsilon_{\mathrm{T}}^{\mu\nu}$, τ_{p0} and E_{p0}. Upon averaging, Equation (38) reduces to Equation (40), which is the product between the characteristic escape rate out of a mega-basin (Equations (5) and (6): the central result of paper I) and the plastic strain average of a heterogeneous volume (Equations (43) and (48)).

(4) When assuming a distribution of barrier energies, paper I and Sections 3–4 found that the characteristic escape rate (Equations (5) and (6)) can be written (Equation (31)) as

$$\sim\text{prefactor} \times \exp\left[-\frac{F(T,\sigma^{\mu\nu})}{k_{\mathrm{B}}T}\right] \tag{56}$$

where $F(T,\sigma^{\mu\nu})$ is termed the free barrier energy which may be formally separated into an internal barrier energy component and a barrier entropy component, that respectively define a temperature dependent apparent barrier energy and a temperature dependent number of accessible structural transformations. Indeed the barrier entropy is directly defined from the barrier energy distribution, therefore giving direct information via Equation (20) on the average number of thermally accessible barriers as a function of temperature. In appendix A of paper I, the viewpoint is also discussed of seeing the entire developed analogy to equilibrium statistical mechanics as simply a change of integration variables in order to evaluate the integral in Equation (16).

(5) In paper I, the prefactor in Equation (56), was *chosen* to have the simple Arrhenius form of $\nu_0 \exp(-E/k_{\mathrm{B}}T)$. This was physically motivated by the α and β time-scales of the under-cooled liquid regime, and that the latter mediates the former. That is, for an amorphous solid multiple reversible thermally activated β activity mediates (via the prefactor) the irreversible α activity, the latter of which facilitates plasticity (see e.g. Ref. [23]). Experimentally there is much evidence that the β time-scale follows a simple Arrhenius behaviour [25,28,53].

(6) Paper I showed that Equation (56) contains two critical stress dependent temperatures: the freezing temperature (when the barrier entropy is zero) and the plastic transition temperature (when the free barrier energy becomes negative). At temperatures below the (lower) freezing temperature a regime of extreme value barrier statistics occurs in which each heterogeneous volume admits only one thermally accessible structural transformation. Above this temperature, the statistics of the most probable dominates allowing for a statistically meaningful average number of available structural transformations. In this latter regime, it is only for temperatures above the (higher) plastic transition temperature, that the number of thermally accessible structural transformations is sufficient to produce a non-negligible plastic transition rate. These transition temperatures are also contained in the present work and will be discussed in further detail in Sections 7 and 8.

Some specific assumptions of the model are now discussed:

(1) The partitioning of the BMG into rigid RVEs is formally only valid under zero load conditions. There however exists much experimental evidence that at temperatures well below the glass transition, BMGs remain homogeneous for both tensile and (simple) compressive loads up to and including yield. Indeed, BMGs exhibit a Weibull modulus comparable to that of crystalline metals indicating that material

failure is well reproduced across different samples [54]. This is strong evidence for homogeneity at a length scale much less than the volume of bulk samples. For deformation experiments exploring plastic flow and ductility beyond yield, the assumption of a rigid RVE clearly breaks down, as does the present assumption that plasticity can be well described via a mean-field description.

(2) The classification of RVE and heterogeneous volumes may be seen as a counting tool with which averages are defined. Indeed, partitioning the structural glass into fundamental units such as the heterogeneous volume avoids the difficult-to-manage continuous degrees of freedom of the atomic scale, and is a simplification that is not new – Stillinger used it for the counting of inherent structures [26]. The statement that an RVE exists is a statement that there are enough heterogeneous volumes to make a statistically meaningful average of Equation (38) when wanting to describe homogeneous plasticity. The RVE could just as well be taken as the volume of a large enough finite system, although the naming convention then becomes inappropriate.

(3) The statement that the plastic rate of a heterogeneous volume is derived from the summation of M individual transition rates (Equation (3) in Section 2) assumes the material can simultaneously sample each exit path. This is an assumption which is related to the definition of M and thus N, and will be investigated in future work. Note also that, because of the extensive nature of the free barrier energy, the size of the heterogeneous volume (the number of atoms N) is not a parameter which greatly effects the resulting homogeneous plasticity, controlling only the sharpness of the freezing and plastic transition temperatures.

(4) It is emphasized that the quantities: internal barrier energy, barrier entropy and free barrier energy are not thermodynamic variables, and instead represent effective kinetic parameters whose transition temperatures (they define) correspond to changes in the average kinetics rather than changes in phase as in the case of equilibrium statistical mechanics. The naming convention is however justified since all three quantities have the same mathematical structure as their thermodynamic counterparts because the characteristic escape rate has the mathematical structure of a partition function – for more details see [36], which also makes a comparison to the corresponding equilibrium thermodynamic quantities.

(5) In producing the mean-field plastic transition rate, Equation (5), the quantities $\varepsilon_{\mathrm{T}}^{\mu\nu}$, τ_{p0} and E_{p0} are assumed to be statistically independent. The assumption is based on the notion that due to the complexity of a structural glass – the diversity of local environments it can admit and the exponential number of available structural transformation – there cannot exist a statistically significant correlation between any of the parameters that characterize a particular escape path realization.

The current work is now compared and discussed in terms of two notable models for glassy systems which also exploit a fixed distribution of energy barriers. In particular, the "trap model" of Bouchaud [55,56] and its later extensions to plastic deformation, the Soft Glass Rheology (SGR) models of Sollich [57,58]. Both models contain a fixed distribution of potential wells (viewed as the states of the system) in which the depth of each well equalled the barrier energy needed to exit it. Each potential well was therefore defined relative to a reference energy above which the system could easily traverse all states of the system. In investigating the potential well statistics, averaging was performed with respect

to sub-systems (c.f. heterogeneous volumes) each containing a set number of potential wells drawn from the fixed distribution.

In the work of Bouchaud, the statistics of trapping times (the time spent within a particular potential well) revealed a critical temperature below which the system spends most of its time in a few deep wells resulting in a divergent mean trapping time and thus a (weak) breaking of ergodicity. In terms of an experiment, this entails that the mean trapping time is comparable to the time spent observing the system. On the other hand, above this critical temperature the mean trapping time is always much smaller than the observing time. This behaviour also results in the familiar "plateau" signature in (this case) the two-time correlation function associated with the probability that the system has not changed it trap [56]. Such results are due to the dominance of extreme value statistics at a sufficiently low temperature, and is very similar to the original freezing work of Derrida in his Random Energy Model [41], and thus the kinetic freezing temperature encountered in paper I and the present work.

There are however important differences between the present work and that of the trap model. The present work only considers the statistics of the barrier energy between mega-basins with the absolute energy at the bottom of each mega-basin being equal. Thus, the critical (freezing) temperature of the present work is not connected to a change in statistics of how the system attempts to approach its most relaxed state. This aspect is implicitly lost in the present coarse-graining, with the view that for plastic evolution the dominating factor is how much of the alpha energy landscape is thermally accessible with the kinetic freezing temperature being the transition temperature below which each heterogeneous volume has on average one dominant thermally accessible barrier. Moreover, it is the plastic transition temperature (when there is a sufficient number of thermally accessible barrier energies for non-negligible plasticity to occur) that can be ascribed to the glass transition temperature – see the subsequent section in which the model is applied to experimental data. In the case of the trapping model, such a connection between barrier height and potential well depth does exist, and the critical transition temperature can be compared to the glass transition temperature.

The SGR model [57,58] extends the trap model of Bouchaud to deformation and plastic flow. Following Ref. [56] the differential equation determining the time dependent probability of a sub-system being in a potential well of depth E is extended to a similar equation dictating the probability of the sub-system being in a potential well of depth E and having the strain state l [57,58]. A critical difference between the SGR model and the present work immediately becomes apparent in that the deformation of the former is driven in part by the system's desire to relax as the deformation proceeds. This is entirely absent in the current mean-field description (since each mega-basin has the same absolute energy value), although Section 8 does discuss the possibility that such effects might be present in Equation (38) (which includes an elastic interaction between heterogeneous volumes) via an evolving internal stress field which could be viewed as the theory's so-called state-variable of plastic evolution.

In fact, because of the connection between barrier height and absolute potential energy, the deformation properties of the SGR model exhibits distinct regimes of behaviour when either below or above the glass transition temperature. Indeed, the flow stress vs. strain rate exhibits a weak strain rate sensitivity below the glass transition temperature, and with increasing temperature transits to a non-Newtonian flow regime and eventually to

a Newtonian flow regime. These latter features are also seen in the mean-field equations of the present model (see paper I and the following section).

A further difference is that the SGR model, like that of STZ theory [2], is athermal where an effective temperature arises from fluctuations due to the inherent quenched disorder within the system. This poses the question of what is the fundamental origin of the timescale during plastic deformation. In Ref. [58], one proposal is that the athermal attempt rate originates from underlying thermally activated local structural transformation akin to that of β relaxation. Such a coarse graining of the microscopic landscape is precisely the approach taken in the present work, where the prefactor of Equation (56) is assumed to have (in this case) a simple Arrhenius form describing the underlying thermally activated β relaxation processes mediating the coarse grained α potential energy landscape.

7. Application to the high-temperature deformation data of Lu et al. [40]

Inspection of Equation (51) reveals the free parameters of the model are $\delta\dot{\gamma}_0$, $\delta\Omega$, and those associated with $E_{\mathrm{p}00} + F(T)$ which are $E_{\mathrm{p}00}$, E_0, δE_0, α and δE_σ. The latter shear stress dependence gets its definition via Equation (42) where here δE_0 is equal to $\delta E_0(\sigma = 0)$. As in paper I, E_0 and δE_0, which define the barrier energy distribution can be entirely determined from experimentally accessible parameters, in particular via the viscosity η_{g} and fragility m at the glass transition temperature T_{g}.

Linear (Newtonian) viscosity may be formally given as

$$\eta_{\mathrm{RVE}} = \lim_{\sigma\to 0} \frac{\sigma}{\dot{\gamma}_{\mathrm{RVE}}} = \frac{k_{\mathrm{B}}T}{\delta\Omega\delta\dot{\gamma}_0} \exp\left[\frac{E_{\mathrm{p}00} + F(T, \sigma = 0)}{k_{\mathrm{B}}T}\right]. \tag{57}$$

One common method to define the glass transition temperature is when the viscosity reaches $\eta_{\mathrm{g}} = 10^{12}$ Pa-sec at a cooling rate of 20 K/min. That is,

$$\eta_{\mathrm{g}} = \frac{k_{\mathrm{B}}T_{\mathrm{g}}}{\delta\Omega\delta\dot{\gamma}_0} \exp\left[\frac{E_{\mathrm{p}00} + F(T_{\mathrm{g}}, \sigma = 0)}{k_{\mathrm{B}}T_{\mathrm{g}}}\right]. \tag{58}$$

In addition to the value of the viscosity at T_{g}, a common material parameter to structural glasses is the fragility – the rate at which viscosity changes with respect to temperature at T_{g},

$$m = \left.\frac{d\log\eta/\eta_0}{d\left(T_{\mathrm{g}}/T\right)}\right|_{T=T_{\mathrm{g}}}. \tag{59}$$

Substitution of Equation (57) into Equation (59) gives

$$m\log 10 + 1 = \frac{E_{\mathrm{p}00} + E(T_{\mathrm{g}}, \sigma = 0)}{k_{\mathrm{B}}T_{\mathrm{g}}} \tag{60}$$

or the internal barrier energy at T_{g}

$$E(T_{\mathrm{g}}, \sigma = 0) = k_{\mathrm{B}}T_{\mathrm{g}}\,(m\log 10 + 1) - E_{\mathrm{p}00}. \tag{61}$$

This physically appealing result is general and arises because Equation (20) requires $T\partial S/\partial T = \partial E/\partial T$ or equivalently the expression, $U/T^2 = \partial(F/T)/\partial T$, which is analogous to the Gibbs–Helmholtz equation in thermodynamics. Further substitution of

Equation (61) into Equation (58), gives the barrier entropy at T_g

$$S(T_g, \sigma = 0) = k_B \left(m \log 10 + 1 - \log \left[\frac{\eta_g \delta\Omega \delta\dot{\gamma}_0}{k_B T_g} \right] \right). \tag{62}$$

Thus, the experimental parameters η_g, m define the free barrier energy at T_g for a given choice of $\delta\Omega$, $\delta\dot{\gamma}_0$ and α. Equations (61) and (62) in conjunction with Equations (29) and (30) also uniquely determine E_0 and δE_0,

$$E_0 = E(T_g, \sigma = 0) \exp \left[- \frac{2 \left(S(T_g, \sigma = 0) - k_B \alpha \right)}{E(T_g, \sigma = 0)} \right] \tag{63}$$

and

$$\delta E_0 = E_0 \sqrt{\frac{k_B T_g}{E(T_g, \sigma = 0)} \log \left[\frac{E_0}{E(T_g, \sigma = 0)} \right]}. \tag{64}$$

It is noted that the time rate of change of viscosity at the glass transition is given as $\dot{\eta}_g = \eta_g m \mathrm{CR} / T_g$ where CR is the cooling rate from the under-cooled liquid regime. Thus, the cooling rate does not give additional information about the theory and emphasizes the fact that the current thermal activation approach is not applicable to the physics of the under-cooled liquid regime.

The remaining free parameters are $\delta\dot{\gamma}_0$, $\delta\Omega$, E_{p00}, α and δE_σ. E_{p00} can be determined from dynamical mechanical analysis or differential scanning calorimetry experiments [24] and the rest from steady state strain rate vs. stress data as a function of temperature, a common data-set used to fit to the Arrhenius form of Equation (55). For Vitreloy-1, such a data-set is found in the work of Lu et al. [40]. For this structural glass initial estimates of $T_g = 623$ K, $m = 40$ and $E_{p00} = 1.4$ eV are taken from both Lu et al. [40] and Wang [24].

Figure 2(a) plots the experimental steady state strain rate vs. stress for a number of temperatures close to and above the glass transition temperature. Following Schuh et al. [1] and Wang [24] it is this data to which the current model (Equation (51)) will be fitted with all parameters allowed to vary. The experimental data is taken from uniaxial compression tests and for conversion between the strain rate and uni-axial stress to the appropriate shear quantities, the former is multiplied by $\sqrt{3}$ and the latter is divided by $\sqrt{3}$. This is motivated by Figure 2(b), which plots Lu's linear viscosity (Figure 8 of Ref. [40]) data multiplied by the shear strain rate and divided by the shear stress. Such numerical factors are common and represent an effective angle of dominant slip activity in a uni-axial deformation experiment, see for example Kawamura et al. [59]. As expected, for a wide range of low shear stresses, the experimental data in Figure 2(b) has converged to approximately unity indicating a stress independent Newtonian viscosity coefficient. The solid curves in Figure 2(a) and (b) indicate a fit of the model obtained via the simulated annealing global minimization algorithm [60]. The corresponding parameters of this fit are $T_g \simeq 621.5$ K, $m \simeq 38.7$, $E_{p00} \simeq 1.44$ eV, $\delta\dot{\gamma}_0 \simeq 2.95 \times 10^9$ sec^{-1}, $\delta\Omega \simeq 1.99 \times 10^{-29}$ m^3, $\alpha \simeq 107.6$ and $\delta E_\sigma \simeq 2.98$ eV, with η_g fixed at 10^{12} Pa-sec.

It is noted that for these parameters, the numerator of Equation (49) evaluated at T_g equals $\simeq 1.03$ for $V_0 \simeq 10$ nm^3, justifying the ensuing approximation of Equation (49).

When interpreted as an activation volume, the parameter $\delta\Omega$ has a numerical value that is similar to that found in Refs. [1,24] when using the Arrhenius form of Equation (55). When assuming that the volume of the heterogeneous volumes is one to three orders of

magnitude larger than this "activation volume", Equations (52) and (53) together with the numerical value of $\delta\dot{\gamma}_0$ indicate a value for τ_{p00} ranging somewhere between 10^9 to 10^{12} – a range of values compatible with it being some multiple of the Debye frequency of the system. The numerical value of δE_σ indicates a weak stress dependence of the distribution of barrier energies, a consequence of which is that the apparent barrier energy has a weak stress dependence and therefore a value ($E(T_g) + E_{p00} \simeq 4.82$ eV) differing little from the activation energy obtained when using Equation (55), which is $Q \simeq 4.6$ eV [1,24]. Indeed for the current parametrization, the stress dependence of the barrier energy distribution has a negligible effect when compared with that associated with the choice of the final mega-basin (the first factor in Equation (40)) – a situation quite different to that encountered in paper I. The corresponding log-normal barrier energy parameters have values of $E_0 = 15.02$ eV and $\delta E_0 = 2.3$ eV indicating that in the high-temperature regime, the relevant part of the distribution ($\sim k_B T_g$) remains that of low-barrier energy tail.

Figure 2(c) displays experimental uni-axial deformation curves at a temperature of 643K for a number of different strain rates. The data are taken directly from Figure 2 of Ref. [40]. The higher strain rate curves are characterized by an initial rise in stress that may be loosely associated with the elastic deformation regime, a peak stress indicating the onset of a material instability and an eventual steady state flow regime. Appendix B of paper I used a simple method to obtain a constant strain rate stress–strain curve from Equation (51), resulting in the stress at time $t + \Delta t$ being given by

$$\sigma(t + \delta t) = \sigma(t) + Y\left[\dot{\varepsilon}_{total}\delta t - \int_t^{t+\delta t} dt\, \dot{\varepsilon}_p(T, \sigma(t))\right]. \tag{65}$$

For a small enough time interval, this may be approximated as

$$\sigma(t + \delta t) = \sigma(t) + Y\dot{\varepsilon}_{total}\delta t\left[1 - \frac{\dot{\varepsilon}_p(T, \sigma(t))}{\dot{\varepsilon}_{total}}\right] \tag{66}$$

and iterated to generate a stress–strain curve.

In the above, the plastic strain rate $\dot{\varepsilon}_p(T, \sigma)$ is given by $\sqrt{3}\dot{\gamma}_{RVE}(T, \sigma)$ (Equation (51)), Y is the appropriate bulk Young's modulus and $\dot{\varepsilon}_{total}$ the chosen constant total strain rate. Using this model, Figure 2(c) also displays the resulting model stress–strain curves. Whilst the steady state stress regime is well described by the model, particularly for low values of strain rate, the peak stress regime associated with the emergence of a stress overshoot is not at all present – a result due to the mean-field nature of the current plasticity model, which necessarily can only describe homogeneous plasticity. Figure 2(d) now shows the experimental peak stress values of Lu et al. [40] for different strain rates as a function of temperature (shown as open circles in the figure). With T_g at approximately 623 K, such data clearly show the transition from a high temperature/low strain rate homogeneous plasticity to a low temperature/high strain rate regime of deformation. Whilst the model is unable to reproduce the peak stress behaviour it is revealing to plot on this curve the temperature dependence of the steady state stresses for comparable strain rates (solid curves). For the lowest strain rate, good agreement is seen in the high temperature regime where experimentally the peak stress regime is absent. For larger strain rates, the quantitative agreement reduces due to the mean-field nature of the current plasticity model – however qualitatively the trends are similar. For this very same reason, the rapid change in experimental behaviour seen as the temperature reduces is not evident in the model, although at higher stresses (beyond the range of the figure) the predicted steady state stress does limit to a plateau with

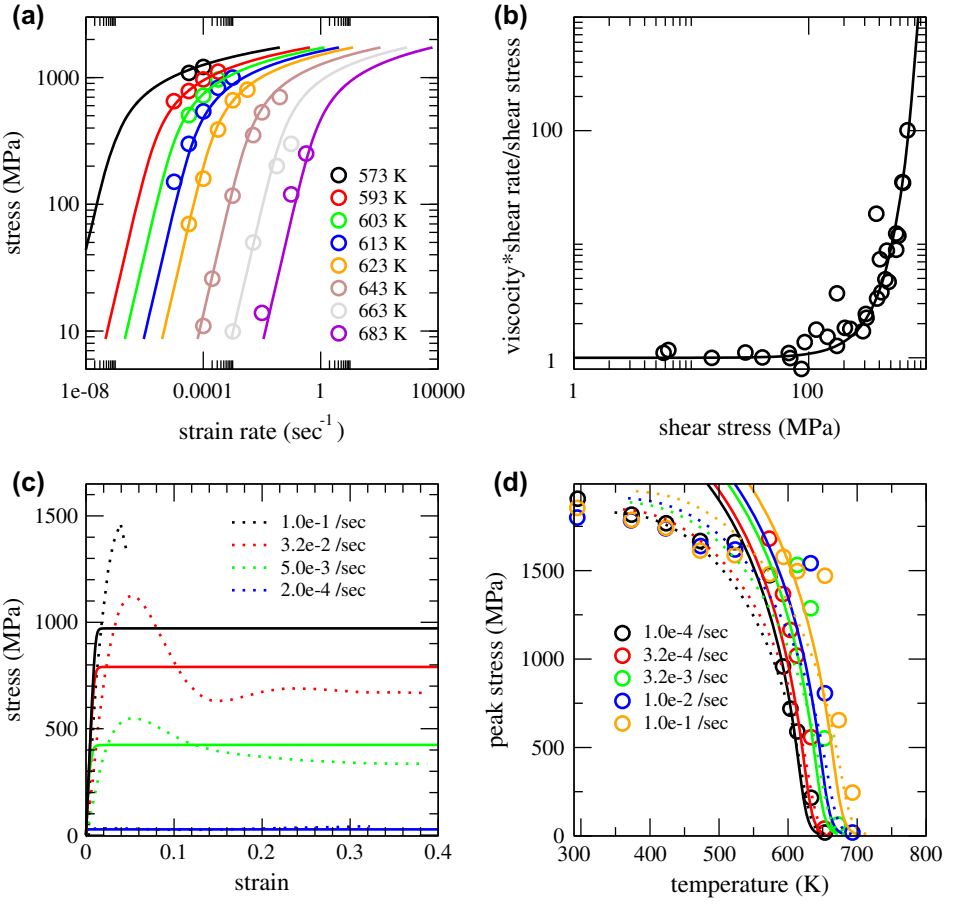

Figure 2. (colour online) For Vitreloy-1, data of (a) steady state strain rate vs. stress, (b) Newtonian viscosity multiplied by shear strain rate and divided by shear stress, (c) uniaxial stress–strain curves for various strain rates at a temperature of 643 K and (d) peak stress as a function of temperature. The symbol (or dashed lines in (c)) data display the experimental data of Lu et al. [40] and the solid curves of similar colour display the corresponding model fit. In (d) the dashed curves represent the model trends when fitted directly to the experimental peak stress data of (c).

a weak temperature dependence – a regime that was investigated in Paper I (see Figure 8 of [36]).

Having said the above, Figure 2(d) also includes (the dashed lines) the consequences of the model when fitted to the peak stress data, as in paper I, rather than the steady state data. The emerging plateau region at low temperatures now becomes evident, although the sharper transition to this temperature regime seen when using the modified Gaussian of paper I is no longer evident when using the more restrictive log-normal distribution of barrier energies. The parameters of this fit are $T_g \simeq 625.0$, $m \simeq 35.1$, $E_{p00} \simeq 1.44$ eV, $\delta\dot{\gamma}_0 \simeq 7.15 \times 10^9$ sec^{-1}, $\delta\Omega \simeq 2.40 \times 10^{-29}$ m^3, $\alpha \simeq 119.7$ and $\delta E_\sigma \simeq 6.25$ eV. These values do not differ substantially from those associated with the fit to steady state flow stress data. The corresponding log-normal barrier energy parameters have values of

$E_0 = 32.5$ eV and $\delta E_0 = 6.7$ eV which represents a distribution that is closer in position to the fitted modified Gaussian distribution used in paper I (see Figure 7c of [36]). Whilst such an approach is certainly not justified in the temperature regime where there is a cross-over from homogeneous to heterogeneous plasticity, and a strong difference between the peak stress and flow stress, well below the glass transition temperature there is little experimental distinction between these stresses. Thus, one could argue (as was done in paper I) that mean field would be applicable both to the quite low temperature and high temperature deformation modes for the onset of plastic deformation (that is yield), with the intermediate cross-over regime not being well described. The dashed curves in Figure 2(d) tend to support this conclusion.

8. Discussion and concluding remarks

The present thermal activation theory provides an entirely kinetic interpretation of the fragility index at the glass transition temperature. This may be seen by writing the barrier entropy, Equation (62), as

$$S(T_g) + k_B \log\left[\frac{\eta_g \delta\Omega \delta\dot{\gamma}_0}{k_B T_g}\right] = k_B\,(m \log 10 + 1)\,. \tag{67}$$

or rather as

$$S(T_g) + k_B \log\left[\frac{\tau_{Exp}}{\tau_{p00}}\right] = k_B\,(m \log 10 + 1)\,. \tag{68}$$

with $\tau_{Exp} = \eta_g V_0 \delta\gamma^2/\left(2k_B T_g\right)$ being viewed as the characteristic experimental time scale associated with the deformation experiment (see paper I). If τ_{Exp} were equal to the fundamental time scale of the β-relaxation modes, τ_{p00}, then $S(T_g)$ would equal $m \ln 10 + 1$ where m is the correspondingly measured fragility. In this limit, the fragility is therefore a direct measure of the apparent number of structural transformations available to each heterogeneous volume element at T_g, that is, $S(T_g)/k_B = \alpha_{App}(T) = m \log 10 + 1$. An analogous identification has also been proposed between fragility and the configurational entropy of the under-cooled liquid PEL by Sastry [27]. This present result immediately implies that α cannot be less than $m \ln 10 + 1$ since $S(T)/k_B < \alpha$ (Equation (23)). Note that, like the barrier entropy, the fragility is an extensive quantity.

For a realistic deformation experiment, $\tau_{Exp} \gg \tau_{p00}$, resulting in the above equality between $S(T_g)$ and m being an over estimation of the barrier entropy. This is because over the period of time, τ_{Exp}, significant *experimentally unresolvable* activity occurs which also contributes to the correspondingly measured fragility. Through the term $k_B \ln\left[\tau_{Exp}/\tau_{p00}\right]$, this activity contributes to an effective reduction of the needed barrier entropy. Thus, when the glass transition is viewed as an entirely kinetic phenomenon (as is done here), the fragility becomes a direct measure of the apparent number of available α-mode structural transformations. Thus, Equation (68) (and Equation (62)) is considered more fundamental than the more familiar Equation (61) which (here) arises from the requirement that the temperature T defined via Equation (20) corresponds to the thermodynamic temperature of the system.

Using the fitted parameters of Vitreloy-1 obtained in Section 7, the value of the ratio $\tau_{Exp}/\tau_{p00} \simeq 3 \times 10^{13}$ suggests a reasonable choice of τ_{p00} (in the range of 10^{-9} to 10^{-12} sec) will give a τ_{Exp} that is within the domain of a typical deformation experiment.

The current mean-field description of macroscopic plasticity is only suited to purely homogeneous plasticity, where within one RVE, it is valid to describe the plasticity as arising from the average response of a heterogeneous volume. Whilst this might be valid for a broad range of temperatures in the flow stress regime, Figure 2(c) and (d) demonstrates that for high enough strain rate or low enough temperature, the mean-field approximation is unable to describe the presumably heterogeneous transition from elasticity to macroscopic plasticity seen in experiment. Indeed at quite low temperatures, where the available number of structural transformations per heterogeneous volume approaches unity a new regime of strongly heterogeneous statistics emerges associated with that of the extreme value. The average temperature at which this occurs is referred to as the kinetic freezing temperature and may be found as the solution to the barrier entropy equalling zero, $S(T_{\rm f}) = 0$: the case when there exists, on average, one available structural transformation per heterogeneous volume. Using Equation (30) and the known properties of the Lambert W-function, this temperature is found to be

$$T_{\rm f}(\sigma) = \frac{1}{k_{\rm B}} \frac{\delta E_0(\sigma)}{\sqrt{2\alpha}} \exp\left[-\sqrt{2\alpha} \frac{\delta E_0(\sigma)}{E_0} \right]. \tag{69}$$

for the log-normal distribution. A Gaussian distribution gives a similar result, but without the exponential factor.

For $T < T_{\rm f}(\sigma)$, the free barrier energy becomes independent of temperature equalling $F(T_{\rm f}(\sigma), \sigma) = E(T_{\rm f}(\sigma), \sigma)$. When sampling the N' heterogeneous volumes of the RVE, the kinetic freezing temperature will fluctuate around this value due to fluctuations in the corresponding kinetic freezing barrier energy, the statistics of which is set by the extreme value Weibull distribution [61]. In this temperature regime, a heterogeneous volume element may contain no accessible barriers below a particular energy threshold allowing for the possibility that no thermally activated structural transformation occurs. It is only in this temperature regime that a single structural transformation associated with a single barrier energy is formally valid. This scenario is quite different from that of the statistics of the most probable, occurring at higher temperatures, where on average there exists a large number of accessible barrier energies resulting in a statistically meaningful average plastic transition rate for each heterogeneous volume. For Vitreloy-1, the parameters of Section 7 give $T_{\rm f} \simeq 191$ K indicating that below room temperature this strongly heterogeneous regime of statistics begins to dominate. When using the numerical values of the model parameters derived from a fit to the peak stress, the freezing temperature rises to approximately 203 K, which is somewhat smaller than that obtained when using a Gaussian distribution fitted also to the peak stress (as done in paper I).

Figure 3 plots the temperature dependence of the free barrier energy, internal barrier energy and barrier entropy for the flow stress parameters of Vitreloy-1. Both the internal barrier energy and barrier entropy reduce with temperature, until the latter becomes zero at the freezing temperature, $T_{\rm f}$. Below this temperature range both quantities become constants independent of temperature. The corresponding free barrier energy shown in Figure 3(a) is negative above a temperature regime associated with the glass transition, and rises when the temperature is lowered. According to Equation (6), in the temperature regime where the free barrier energy is positive, the plastic rate reduces many orders of magnitude when compared to the value associated with the glass transition temperature regime. At $T < T_{\rm f}$, the free barrier energy also becomes constant, and it is in this regime a simple temperature independent value for both the number of available structural transformations

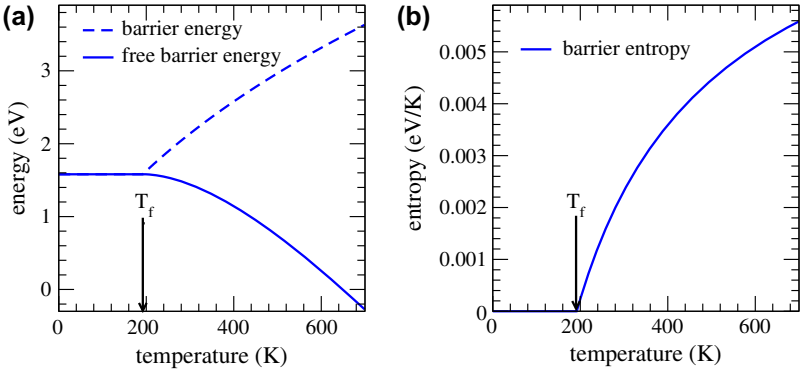

Figure 3. (colour online) (a) Plot of free barrier energy and internal (apparent) barrier energy, and (b) barrier entropy as a function of temperature for the Vitreloy-1 parameterization. Indicated is the freezing temperature, T_f, below which the barrier entropy is zero and on average there exists one available structural transformation within each heterogeneous volume, resulting in the free energy and barrier energy becoming temperature independent quantities for $T < T_f$.

and the energy barrier is formally justified. Despite this, the work of Section 7 demonstrates that temperature independent quantities can be used to describe reasonably well the high temperature/homogeneous deformation regime. Indeed, Figure 3 demonstrates that both barrier energy and entropy do not vary greatly over the 550 K to 650 K temperature range.

The mean-field form for the shear strain rate, Equation (54), is operationally similar to the well-known Arrhenius form (Equation (55)) and justifies the so-called critical barrier energy alluded to by Argon [4] and Johnson and Samwer [5]. Indeed, in paper I, the fluctuations around the apparent barrier energy where shown to scale as $1/\sqrt{N}$. Despite this similarity, there exist some fundamental differences between the present model and the earlier thermal activation models. The Arrhenius shear strain rate is assumed to be proportional to the fraction of volume in which structural transformations can take place [1]. The present theory and Equation (54) also gives a plastic shear rate that is proportional to the number of available structural transitions, $\exp(S(T)/k_b)$, however this number scales exponentially with atom number and therefore volume. Since this number can be rather large, the traditional athermal concept of a dilute density of (liquid like) regions existing within the structural glass which are amenable to plastic deformation has been abandoned – in the present work, any particular region of the material can admit a very large number and variety of structural transformations. Of course, at low enough T, the apparent number of structural transformations drastically reduces as the entire α-relaxation PEL gradually freezes out and the kinetic freezing regime is entered.

Another similarity between Equations (54) and (55) is a shear stress dependent term which for the present work has the form $x\exp(x^2)(\mathrm{I}_0[x^2]+\mathrm{I}_1[x^2])$ and for the Arrhenius form is $\sinh(x)$. In both cases, $x = \text{Volume}\times\sigma/(k_bT)$. For the Arrhenius form, the volume term is seen as an activation volume associated with the barrier enthalpy of the volume distortion needed for the structural transformation to occur. In the present work, this quantity originates from the variance of the distribution of available local plastic strains, $\delta\gamma$, via $\delta\Omega = V_0\delta\gamma/2$. The right-hand side of this equality may be seen as a measure of the variance of the available slipped volume within the system, which itself is coming from a characteristic internal slipped area multiplied by a characteristic slip distance.

In Equation (55), the $\sinh(x)$ factor arises from reversibility of the single characteristic structural transformation of the system and that the sign of the enthalpy term changes for the inverse process. For the present work, the factor $x\exp(x^2)(\mathrm{I}_0[x^2]+\mathrm{I}_1[x^2])$ in Equation (54) is due to a quite different reason where each transition to a new mega-basin results in the material on average having once again access to all possible plastic transitions. Thus although the reverse transition is allowed, it will occur with negligible probability, since it must compete with all other accessible α structural transformations. The factor $x\exp(x^2)(\mathrm{I}_0[x^2]+\mathrm{I}_1[x^2])$ then arises from the mean-field average (integration) over all possible plastic transitions.

Whilst the currently developed mean-field picture affords some insight into the consequences of the present theory to macroplasticity, it certainly is limited to the low strain rate and high temperature range, a regime that is experimentally insensitive to fluctuations away from homogeneity, and also to the thermal and loading history of the material. Indeed, inherent to the above picture is that the material has no memory of its past state. This is direct result of the mean-field theory variant presently used since the elastic interaction between heterogeneous volumes is not at all considered. When such interactions are taken into account, the pre-history of the material will play an integral role in its response to an external condition. In this regard, the internal stress field may be viewed as the state-variable of the model. To address these aspects of low temperature, high strain rate and material history, the mean-field approach must be abandoned and an approach which considers correlated spatial variations in plastic activity must be considered. How to develop a theory of macroscopic plasticity beyond mean-field, and which spans the regime of T_{f} up to T_{g} for experimentally accessible strain rates, will be the subject of paper III in this series of work.

Acknowledgements

The authors wish to thank D. Rodney, K. Samwer and J.-P. Bouchaud for helpful discussions. R.M. thanks C.A. Volkert for institutional support.

Note

1. If such a Eshelby construction were to be performed, the associated deformation and relaxation would clearly need to be atomically constrained in order to maintain the saddle-point configuration.

References

[1] C.A. Schuh, T.C. Hufnagel and U. Ramamurty, Acta. Mater. 55 (2007) p.4067.
[2] M.L. Falk and J.S. Langer, Ann. Rev. Condens. Matter Phys. 2 (2011) p.353.
[3] F. Spaepen, Acta Metall. 25 (1977) p.407.
[4] A. Argon, Acta Metall. 27 (1979) p.47.
[5] W.L. Johnson and K.A. Samwer, Phys. Rev. Lett. 95 (2005) p.195501.
[6] M.H. Cohen and D. Turnbull, J. Phys. Chem. 31 (1959) p.16.
[7] D. Turnbull and M.H. Cohen, J. Phys. Chem. 34 (1961) p.120.
[8] D. Turnbull and M.H. Cohen, J. Phys. Chem. 52 (1970) p.3038.
[9] M.L. Falk and J.S. Langer, Phys. Rev. E 57 (1998) p.7192.
[10] C.A. Schuh and A.C. Lund, Nat. Mater. 2 (2003) p.449.

[11] C.E. Maloney and A. Lemaître, Phys. Rev. Lett. 93 (2004) p.016001.
[12] M.J. Demkowicz and A.S. Argon, Phys. Rev. Lett. 91 (2004) p.025505.
[13] Y. Shi and M.L. Falk, Phys. Rev. B 73 (2006) p.214201.
[14] P. Guan, M. Chen and T. Egami, Phys. Rev. Lett. 104 (2010) p.205701.
[15] M.J. Demkowicz and A.S. Argon, Phys. Rev. B 72 (2005) p.245205.
[16] M.J. Demkowicz and A.S. Argon, Phys. Rev. B 72 (2005) p.245206.
[17] J.S. Langer, Phys. Rev. E 77 (2008) p.021502.
[18] D.E. Bouchbinder, J.S. Langer and I. Procaccia, Phys. Rev. E 75 (2007) p.036107.
[19] M.L. Falk, J.S. Langer and L. Pechenik, Phys. Rev. B 70 (2004) p.011507.
[20] J.S. Langer, Phys. Rev. E 70 (2004) p.041502.
[21] M. Goldstein, J. Chem. Phys. 51 (1969) p.3728.
[22] C.A. Angell, K.L. Ngai, G.B. McKenna, P.F. McMillan and S.W. Martin, J. Appl. Phys. 88 (2000) p.3113.
[23] J.S. Harmon, M.D. Demetriou, W.L. Johnson and K. Samwer, Phys. Rev. Lett. 99 (2007) p.135502.
[24] W.H. Wang, J. Appl. Phys. 110 (2011) p.053521.
[25] F.H. Stillinger, Science 267 (1995) p.1935.
[26] F.H. Stillinger, Phys. Rev. E 59 (1999) p.48.
[27] S. Sastry, Nature 409 (2001) p.164.
[28] P.G. Debenedetti and F.H. Stillinger, Nature 419 (2001) p.259.
[29] M. Scott Shell, P.G. Debenedetti and A.Z. Panagiotopoulous, Phys. Rev. Lett. 92 (2004) p.035506.
[30] Y.V. Fyodorov, Phys. Rev. Lett. 92 (2004) p.240601.
[31] G. Adam and J.H. Gibbs, J. Chem. Phys. 43 (1965) p.139.
[32] T.R. Kirkpatrick, D. Thirumalai and P.G. Wolynes, Phys. Rev. A 40 (1989) p.1045.
[33] A. Heuer, J. Phys.: Condens. Matter 20 (2008) p.373101.
[34] P.M. Derlet and R. Maaß, Phys. Rev. B (RC) 84 (2011) p.220201.
[35] P.M. Derlet and R. Maaß, Mater. Res. Soc. Symp. Proc. 1520 (2012) p.mrsf12-1520-nn07-06, doi:10.1557/opl.2012.1689.
[36] P.M. Derlet and R. Maaß, Phil. Mag. 93 (2013) p. 4232.
[37] D. Klaumünzer, R. Maaß, F.H. Dalla Torre and J.F. Löffler, Appl. Phys. Lett. 96 (2010) p.061901.
[38] R. Maaß, D. Klaumüzer and J.F. Löffler, Acta Mater. 59 (2011) p.3205.
[39] R. Maaß, D. Klaumüzer, G. Villard, P.M. Derlet and J.F. Löffler, Appl. Phys. Lett. 100 (2012) p.071904.
[40] J. Lu, G. Ravichandran and W.L. Johnson, Acta Mater. 51 (2003) p.3429.
[41] B. Derrida, Phys. Rev. Lett. 45 (1980) p.79.
[42] J.D. Eshelby, Proc. Roy. Soc. A 241 (1957) p.376.
[43] T. Mura, *Micromehanics of Defects in Solids*, Martinus Hijhoff, The Hauge, 1982.
[44] V.V. Bulatov and A.S. Argon, Model. Simul. Mater. Sci. Eng. 2 (1994) p.167.
[45] V.V. Bulatov and A.S. Argon, Model. Simul. Mater. Sci. Eng. 2 (1994) p.185.
[46] V.V. Bulatov and A.S. Argon, Model. Simul. Mater. Sci. Eng. 2 (1994) p.203.
[47] E.R. Homer and C.A. Schuh, Acta Mater. 57 (2009) p.2823.
[48] E.R. Homer and C.A. Schuh, Model. Simul. Mater. Sci. Eng. 18 (2010) p.065009.
[49] L. Li, E.R. Homer and C.A. Schuh, Acta Mater. 61 (2013) p.3347.
[50] D. Rodney and C.A. Schuh, Phys. Rev. Lett. 102 (2009) p.235503.
[51] D. Rodney and C.A. Schuh, Phys. Rev. B. 80 (2009) p.184203.
[52] P. Koziatek, J.-L. Barrat, P.M. Derlet and D. Rodney, Phys. Rev. B 87 (2013) p.224105.
[53] G.P. Johari and M. Goldstein, J. Chem. Phys. 53 (1970) p.2372.
[54] W.F. Wu, Y. Li and C.A. Schuh, Phil. Mag. 88 (2008) p.71.
[55] J.P. Bouchaud, J. Phys. I 2 (1992) p.1705.
[56] C. Monthus and J.P. Bouchaud, J. Phys. A 29 (1996) p.3847.

[57] P. Sollich, F. Lequeux, P. Hébraud and M.E. Cates, Phys. Rev. Lett. 78 (1997) p.2020.
[58] P. Sollich, Phys. Rev. E 58 (1998) p.738.
[59] Y. Kawamura, T. Nakamura and A. Inoue, Scripta Mat. 39 (1988) p.301.
[60] A. Corana, M. Marchesi, C. Martini and S. Ridella, ACM Trans. Math. Softw. 13 (1987) p.262.
[61] E.J. Gumbel, *Statistics of Extremes*, Dover, New York, 2004.